

## NUMERICAL STUDY AND PERFORMANCE OF A DEW POINT EVAPORATIVE COOLER FOR BUILDINGS IN CONSTANTINE, ALGERIA

D. Abada<sup>1,2,3\*</sup>, D. Rouag-Saffidine<sup>2</sup>, C. Maalouf<sup>3</sup>, G. Polidori<sup>3</sup>, O. Sotehi<sup>2</sup>

<sup>1</sup>Architecture Department, Faculty of Earth Sciences and Architecture, University of Oum El Bouaghi, 04000, Oum El Bouaghi, Algeria

<sup>2</sup>Energy & Environment Laboratory, Faculty of Architecture and Urban Planning, University of Constantine 3, 25016, Ali Mendjeli, Constantine, Algeria

<sup>3</sup>TheMM, University of Reims Champagne-Ardennes, UFR Sciences Exactes et Naturelles, Campus du Moulin de la Housse, BP 1039 51687 Reims Cedex 2, France

Received: 12 May 2020 / Accepted: 14 September 2020 / Published online: 01 January 2021

### ABSTRACT

Due to the ever-growing demand for air-conditioning to bring the indoor air temperature to a comfortable level regardless of the excessive electricity consumption, research is more oriented towards new techniques enabling more energy savings and less adverse environmental impacts. Dew point evaporative cooling systems hold among the most promising because of their ability to reduce the outside air temperature below its wet bulb level while keeping the absolute humidity constant.

The current paper aims to report an investigation, which tackles the cooling capacity of the system under the Algerian Climate. Constantine city (Algeria) climatic data are retained for the modelling and designing of the system in question. The study involves a variation of its length and air return rate interaction with its efficiency and air temperature supply.

**Keywords:** Evaporative Cooling, Dew Point Temperature, Numerical Modeling.

Author Correspondence, e-mail: [djallelabada@gmail.com](mailto:djallelabada@gmail.com)

doi: <http://dx.doi.org/10.4314/jfas.v13i1.31>



**NOMENCLATURE:**

<b>Symbol</b>	<b>Definition</b>	<b>Unit</b>
$C_p$	Specific Heat Capacity at constant pressure	kJ/(kg.K)
$D$	channel width	m
$g$	moisture content	g/kgd
$g_a$	humidity ratio of air	kg/kg <sub>a</sub>
$g_{fw}$	humidity ratio at saturation near water film	kg/kg <sub>a</sub>
$h_{aw}$	heat transfer coefficient in the wet channel	W/m <sup>2</sup> .K
$h_m$	convective mass transfer coefficient between the wet airflow and the water film surface.	W/m <sup>2</sup> .K
$Le$	Lewis number	
$\dot{m}_d$	mass airflow rate in the dry channel.	kg/s
$\dot{m}_a$	mass airflow rate in the wet channel	kg/s
$Q_s$	sensible heat load	kW
$Q_L$	latent heat load	kW
RH	Relative Humidity	%
$T_d$	air dry bulb temperature in the dry channel	°C
$T_{fw}$	water film surface temperature	°C
$t_a$	air-dry bulb temperature in the wet channel	°C
Tdb	dry bulb Temperature	°C
Twb	wet bulb Temperature	°C
Tdp	dew point Temperature	°C
$T_{in}$	inlet Temperature	°C
$T_{out}$	outlet Temperature	°C
Tsupp	Supply Air Temperature	°C
$U_d$	the overall heat transfer coefficient between the dry channel and water film	W/m <sup>2</sup> .K
w	absolute humidity ratio	g/kg

---

$x/L$	Channel Length	%
Subscripts		
$a$	Air	
$aw$	Wet air	
$d$	dry channel	
$db$	dry bulb	
$dp$	dew point	
$fw$	water film	
$in$	Inlet	
$L$	Latent	
$m$	Mass	
$out$	Outlet	
$S$	Sensible	
$wb$	wet bulb	
Greeks symbols		
$\varepsilon_{dp}$	dew point cooling efficiency	
$\varepsilon_{wb}$	wet bulb cooling efficiency	
$\rho$	mass density of humid air	Kg/m <sup>3</sup>
$\Delta T$	Temperature Difference	°C
Abbreviation		
APRUE	Agence Nationale pour la Promotion et la Rationalisation de l'Utilisation de l'Energie	
COP	Coefficient Of Performance	
DEC	Direct Evaporative Cooler	
DPEC	Dew Point Evaporative Cooler	
IEC	Indirect Evaporative Cooler	
SHR	Sensible Heat Ratio	
SPARK	Simulation Problem Analysis and Research Kernel	

## 1. INTRODUCTION

Building sector in Algeria is the largest energy-consuming sector due to either lacking thermal insulation efficient or housing stock aging. As a fact, for the building sector (Tertiary - Residential), the average final energy consumption over ten years was estimated at 43% in 2017 by the APRUE [1]. The same report, confirms that the electricity intake was registered to exceed 69% of the global value. Such a statement is assumed to only worsen with the constantly increasing demand for air conditioning. For instance, in 2014, the rate of households equipped with air conditioners in Algeria was estimated at 16% corresponding to 700 kWh of electricity consumption [2]. Currently, a pilot survey conducted in December 2019 in a sample of residential neighbourhoods in Constantine revealed that out of 209 households, 70% are equipped with air-conditioners. More, the number of these may reach an average 3 units per apartment (Figure.1).



**Fig.1.** Samples of air conditioners implementation in buildings in Constantine (Déc. 2019)

Thus, one major objective of this research was orientated towards the examination of viable alternatives (inspired by traditional air conditioning methods) capable to provide indoor thermal comfort with passive means. Though in practice, most architects would go for more standard building design for merely cost and/or manufacture reasons, the advances in research works have came up with clear evidence that the concept of the evaporative cooling can be energy efficient and a positive contribution to the environment hot and dry climate [3-6].

---

Among the most widely used evaporative systems are the direct and indirect ones that also have some disadvantages like high humidity supply for the direct system or reduced efficiency for the indirect system [7,8]. For both cases, cooling is limited to ambient wet bulb temperatures. Recently, new technologies and materials have broken these barriers by using novel heat exchangers and flow path arrangements so that temperatures below wet bulb temperatures are reached. Such technologies are known as dew point evaporative cooling systems.

In 2003 Maisotsenko, introduced a new design of a heat exchanger for the indirect system [9] in the form of a combination of a cross-flow, multi-perforated flat plate and an evaporative cooler, in which the secondary air is pre-cooled in the dry channel before being deviated and passing through the wet channel. This process allowed also the heat transfer with the dry channel. The primary air temperature is thus lower than air wet bulb temperature and approaches the incoming air dew point. Later, Hasan [10] presented a theoretical model of several configurations of dew point coolers. He concluded that the ultimate temperature at which the supply air can be cooled is its dew point temperature.

Another experimental study related to an evaporative dew point cooler with different air inlet conditions (velocity, humidity, and temperature) [11] showed that the wet bulb effectiveness is high and varies between 92 to 114%. Lee and Lee [12] used counter-current with a wet return surface cooler and showed that temperatures below wet bulb can be achieved. The authors built and tested a prototype with a finned aluminium plate to optimize heat transfer. The results show that for an air inlet temperature of 32°C with a relative humidity of 50%, the outlet temperature of the dry channel is 22°C, which is below the corresponding wet bulb temperature of 23.7°C.

Lin et al. [13] have investigated numerically and experimentally a cross flow dew point evaporative cooler and concluded that:

- For a supply air with moderate humidity the overall wet bulb and dew point effectiveness of the cooler can reach 1.25 and 0.85;
- Under humid ambient condition, the system has the wet bulb effectiveness, cooling capacity and COP equal to 0.86, 2.2 kW and 4.6 respectively;

- The cooling capacity can be improved to 70-135% by the dehumidification of the supply air. Further, a numerical and experimental investigation upon a configuration of a counter-current dew point cooler using a saturated porous media instead of the water film [14], allowed to achieve a system efficiency of the order of 1.024 for a cooling capacity of the order of 225 W.m<sup>-2</sup>. Lin et al. [15] have experimentally studied an evaporative dew point cooler under different operating conditions (supply air conditions, velocity, working air ratio and channel height). The results show that the average convective heat and mass transfer coefficients are in the range of 26.8-29.9 W/(m<sup>2</sup>K) and 0.025-0.027 m/s respectively.

On another hand, Sohani et al. [16] have studied various types and Materials of heat and mass exchangers to find the best design of dew point coolers and set up the statement that the optimal characteristic values such as (velocity, length, height, width,...etc.) were more dependent of the climatic conditions than of the materials cost.

Lin et al. [17] designed and investigated a counter-flow dew point evaporative cooler in both vertical and horizontal orientations. As a result, it was found that the sprayed water has negative effect on the state of the channel plate because it disturbs the temperature distribution on the surface of the channel and that the horizontal orientation is relatively more stable. A product air temperature ranging from 15.9 to 23.3°C and a COP between 8.6 and 27.0 were attained.

In their investigation, involving a comparison of two configurations of a dew point evaporative cooler, one with an inlet air flows parallel to the water film and a second with an inlet air flows in the opposite direction of the water film, Wan et al [18,19] provided evidence that the counter flows configuration has better cooling effectiveness and lower temperature product than the parallel one.

For their part Liu et al. [20], studied a dew-point evaporative cooler with a corrugated surface heat and mass exchanger. They find that the product air temperature and the cooling capacity are influenced by the inlet air conditions (wet-bulb temperature, air flow rate, humidity ratio). Upon the basis of the here above cited various findings, the following investigation is confined to the modelling and validation of the cooling capacity of a dew point evaporative cooler under Constantine Mediterranean continental climatic conditions (North East Algeria;

36.283N 6.617E, Elev.694m) [meteonorm V7.1.11.24422].

This paper concerns a proposal of a mathematical model of a dew point evaporative cooler and its implementation in SPARK [21,22] together with its validation using data from literature [10,11]. A series of simulations are run to study the system parameters variation on its cooling efficiency and air temperature supply under approaching thermal comfort values.

## 2. DESCRIPTION OF THE DEW POINT SYSTEM AND ITS APPLICATION IN BUILDINGS

### 2.1. System Description

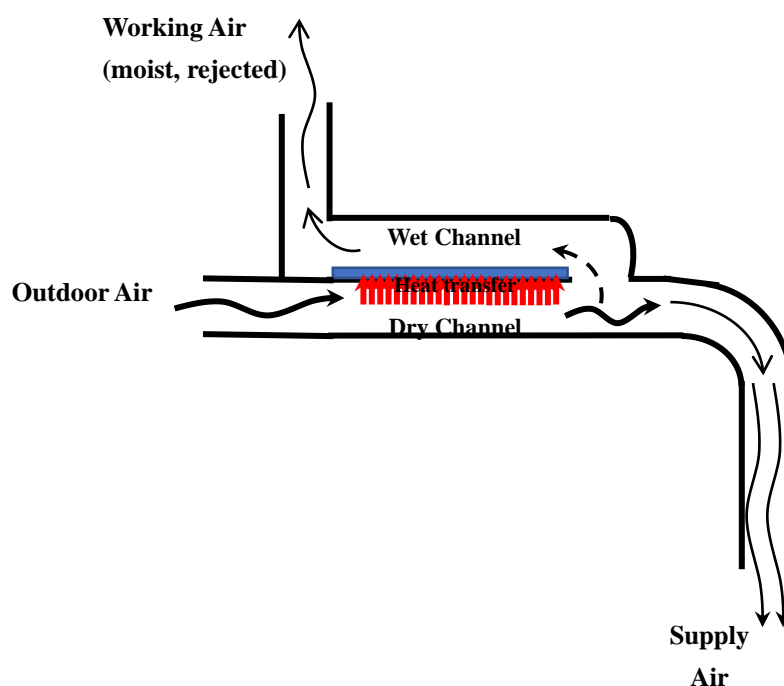


**Fig.2.** Schematic representation of the studied evaporative dew point cooler

The studied dew point evaporative cooler consists of a two-channel (dry and wet) counter-current heat exchanger exchanging heat through a thin wall (Figure.2). The latter is in contact with the air flow in the wet channel through a thin film of water or a saturated wet porous material while it is made impermeable to moisture on its back surface in contact with the dry channel. The outdoor dry air enters the dry channel and loses heat towards the wet channel through the wall separating them. At the end of the dry channel, it is divided into two parts: the dry air which is blown into the conditioned space and the remaining part called working air is

---

diverted into the wet channel, absorbing the heat from the dry channel as well as the moisture evaporates from the wet wall. The ratio of the air flow in the wet channel to that of the dry channel is called the working air ratio and generally varies between 0.3 and 0.7 [23].

## **2.2. Application in Buildings**

Depending on the needs, i.e. as back-up or main equipment for indoor air conditioning, the dew point evaporative cooler could be a stand-alone unit that would be placed individually in a house, a store or office building, or, on the other hand, the system can be integrated in a central unit. This application will allow air to be centrally treated and routed to individual spaces through the pre-set duct system. Depending on the location of the installation, the associated climatic conditions and to ensure precise control of the temperature and humidity of the ambient air, the supply air may require a pre-dehumidification treatment before enter the dew point exchanger, which could be achieved using, for example, a desiccant wheel. This treatment makes it possible to obtain a constant dew point temperature for the supplied air and, subsequently, a constant cooling capacity.

## **3. REVIEW OF CLIMATE CHARACTERISTICS OF THE SITE OF STUDY**

Through four locations; Algiers, Constantine, Setif and Ouargla, representative of the typical environmental conditions encountered in the different Algerian climatic zones as shown in figure 3 (A, B, C, and D respectively) [24,25] summer season weather data were analysed. While the period of June to September is retained for the cities of Algiers, Constantine and Setif, May to October is the period considered for the city of Ouargla located further south.



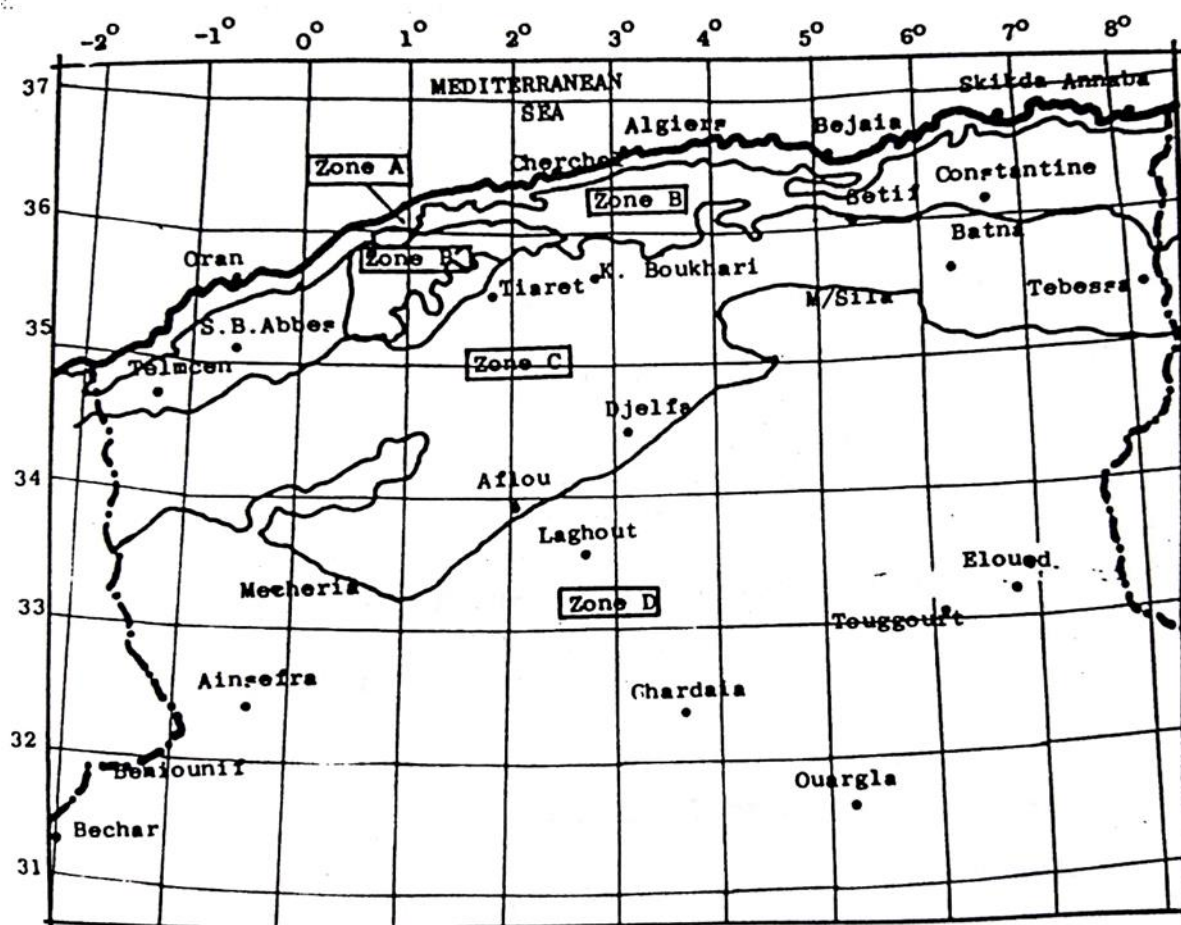


Fig.3. Climatic Zones in Algeria [25]

Then the weather data including dry, wet and dew point temperatures of ambient air of a typical year were examined. Differences between dry and dew point temperatures as well as dry and wet temperatures were calculated. This made it possible to obtain the average, maximum and minimum values of these temperatures, as well as their frequencies occurring in different bands. Three activity patterns i.e. 24h; day and night, were examined and their temperature profiles were generated accordingly.

As previously advanced, Constantine represents the case study of the current work, and therefore the figures 4-6 show its temperature profiles according to the three operating schemes named above (24h; day and night).

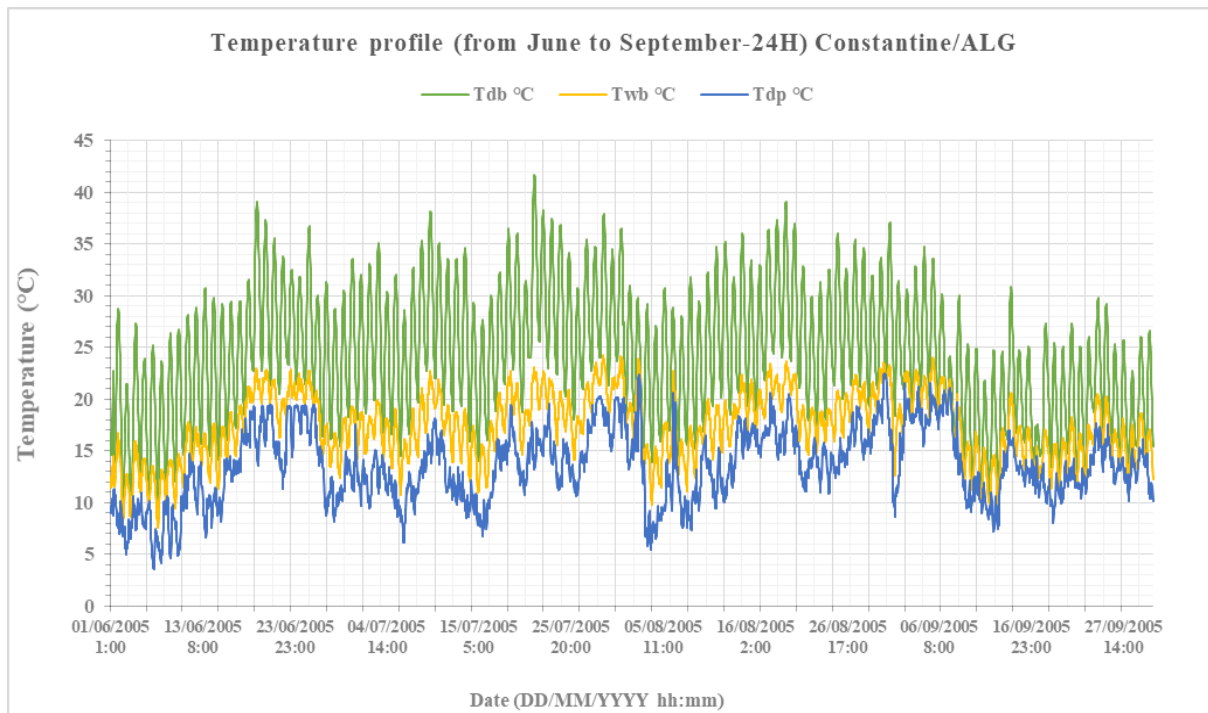


Fig.4. Constantine temperature profile in summer season – 24H

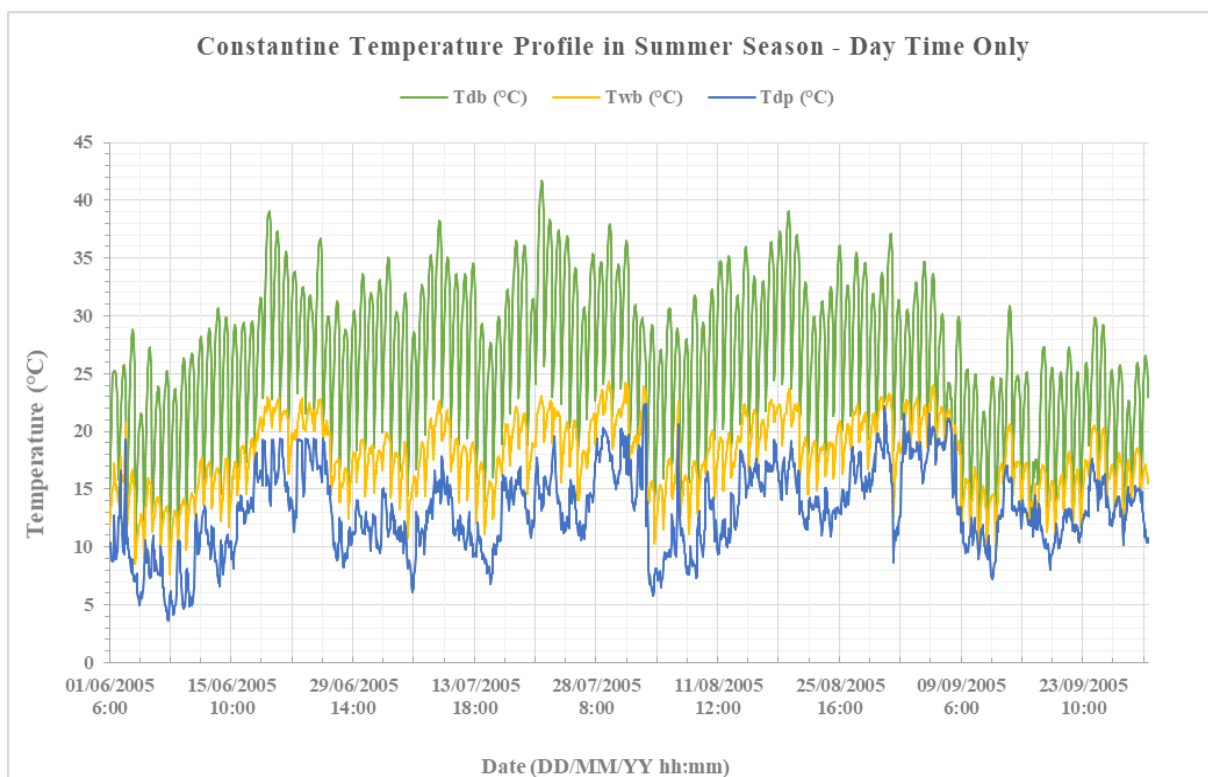
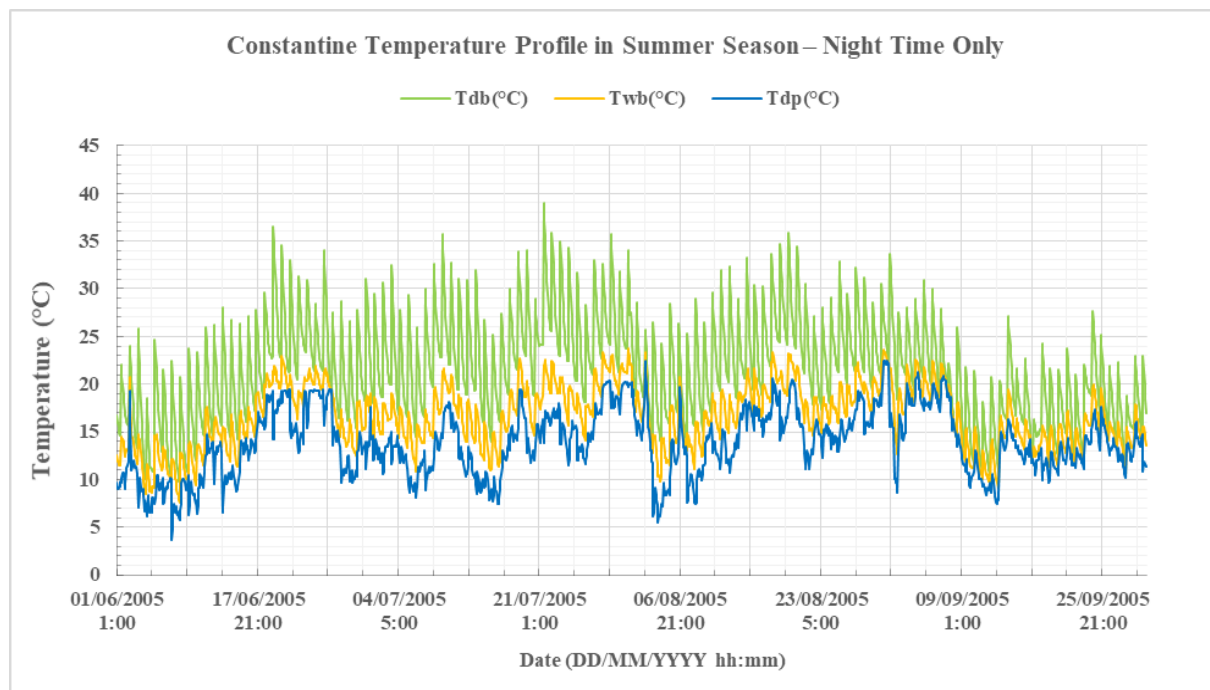


Fig.5. Constantine Temperature Profile in Summer Season – Day Time Only



**Fig.6.** Constantine Temperature Profile in Summer – Night Time only

Meteorological data for the other regions were examined but were not presented here in diagrams. A summary has been given in table.1 for 24h operation.

**Table 1.** Statistic Data of dry bulb and difference between dry bulb and dew point for the selected Algerian Cities (24h operation)

Location	Dry Bulb Temperature (°C)			$\Delta T = Tdb - Tdp$ (°C)		
	Max	Min	Average	Max	Min	average
Alger	39.1	12.1	24.6	17.4	0	6.5
Constantine	41.7	9.8	24.3	28	0	10.8
Sétif	39.9	8.4	23.71	29.4	0	13.48
Ouargla	48.7	13.6	31.43	38.8	2.9	19.9

In fact, during the Constantine hot season, the ambient air temperature is in the range of 9.8 – 41.7°C and its average is 24.3°C (Table 2).

**Table 2.** Statistic Data of dry bulb Temperature and difference between dry bulb and dew point and between dry bulb and wet bulb for Constantine in summer season – 24H.

<b>Dry bulb Temperature (°C)</b>	<b>Number of Hours</b>	<b>percentage %</b>
<5	0	0.00
5-10	2	0.07
10-15	179	6.11
15-20	577	19.71
20-25	865	29.54
25-30	714	24.39
30-35	457	15.61
35-40	129	4.41
40-45	5	0.17
>45	0	0.00
<b>Dry bulb Temperature (°C)</b>		
<b>Min</b>		9.80
<b>Max</b>		41.70
<b>Average</b>		24.30
<b><math>\Delta T = T_{db} - T_{dp}</math> (°C)</b>	<b>Number of Hours</b>	<b>percentage %</b>
<0	0	0.00
0-5	600	20.49
5-10	848	28.96
10-15	651	22.23
15-20	563	19.23
20-25	258	8.81
25-30	8	0.27
>30	0	0.00
<b><math>\Delta T = T_{db} - T_{dp}</math> (°C)</b>		
<b>Min</b>		0.00

<b>Max</b>		28.00
<b>Average</b>		10.80
$\Delta T = T_{db} - T_{wb} (^{\circ}C)$	Number of Hours	percentage %
<0	0	0.00
0	3	0.10
0-2	239	8.16
2-4	570	19.47
4-6	533	18.20
6-8	438	14.96
8-10	389	13.29
10-12	351	11.99
12-14	264	9.02
14-16	125	4.27
16-18	12	0.41
18-20	4	0.14
>20	0	0.00
$\Delta T = T_{db} - T_{wb} (^{\circ}C)$		
<b>Min</b>		0.00
<b>Max</b>		19.20
<b>Average</b>		6.98

In 69.54% of the time, between June and September, the dry air temperature is in the temperature range of 20 – 35°C. The average temperature difference between the dry bulb and the dew point is 10.8°C, which is 3.82°C higher than that between the dry bulb and the wet bulb.

During the day, this average reaches 13.15°C (Table 3), while during the night it gets to 7.86°C (Table 4), which means that a cooling capacity can be attained the day than during the nighttime.

**Table 3.** Statistic Data of dry bulb Temperature and difference between dry bulb and dew point and between dry bulb and wet bulb for Constantine in summer season – Day Time Only.

Dry bulb Temperature (°C)	Number of Hours	percentage %
<5	0	0.00
5-10	1	0.06
10-15	68	3.98
15-20	210	12.30
20-25	415	24.30
25-30	483	28.28
30-35	399	23.36
35-40	127	7.44
40-45	5	0.29
>45	0	0.00
Dry bulb Temperature (°C)		
<b>Min</b>		9.80
<b>Max</b>		41.70
<b>Average</b>		26.34
$\Delta T = T_{db} - T_{dp}$ (°C)	Number of Hours	percentage %
<0	0	0.00
0	2	0.12
0-5	224	13.11
5-10	308	18.03
10-15	414	24.24
15-20	499	29.22
20-25	253	14.81
25-30	8	0.47
30-35	0	0.00

$\Delta T = T_{db} - T_{dp} (^{\circ}C)$		
<b>Min</b>		0.00
<b>Max</b>		28.50
<b>Average</b>		13.15

$\Delta T = T_{db} - T_{wb} (^{\circ}C)$	Number of Hours	percentage %
<0	0	0.00
0	3	0.18
0-2	98	5.74
2-4	196	11.48
4-6	200	11.71
6-8	233	13.64
8-10	276	16.16
10-12	309	18.09
12-14	253	14.81
14-16	124	7.26
16-18	12	0.70
18-20	4	0.23
>20	0	0.00

$\Delta T = T_{db} - T_{wb} (^{\circ}C)$		
<b>Min</b>		0.00
<b>Max</b>		19.20
<b>Average</b>		8.50

**Table 4.** Statistic Data of dry bulb Temperature and difference between dry bulb and dew point and between dry bulb and wet bulb for Constantine in summer season – Night Time

only

Dry bulb Temperature (°C)	Number of Hours	percentage %
<5	0	0.00
5-10	2	0.14
10-15	143	9.77
15-20	423	28.89
20-25	512	34.97
25-30	278	18.99
30-35	98	6.69
35-40	8	0.55
>40	0	0.00
Dry bulb Temperature (°C)		
<b>Min</b>		9.80
<b>Max</b>		41.7
<b>Average</b>		24.30
$\Delta T = T_{db} - T_{dp}$ (°C)	Number of Hours	percentage %
<0	0	0.00
0	2	0.14
0-5	463	31.58
5-10	588	40.11
10-15	273	18.62
15-20	116	7.91
20-25	23	1.57
25-30	1	0.07
>30	0	0.00



$\Delta T = T_{db} - T_{dp} (^{\circ}C)$		
<b>Min</b>		0.00
<b>Max</b>		25.2
<b>Average</b>		7.86

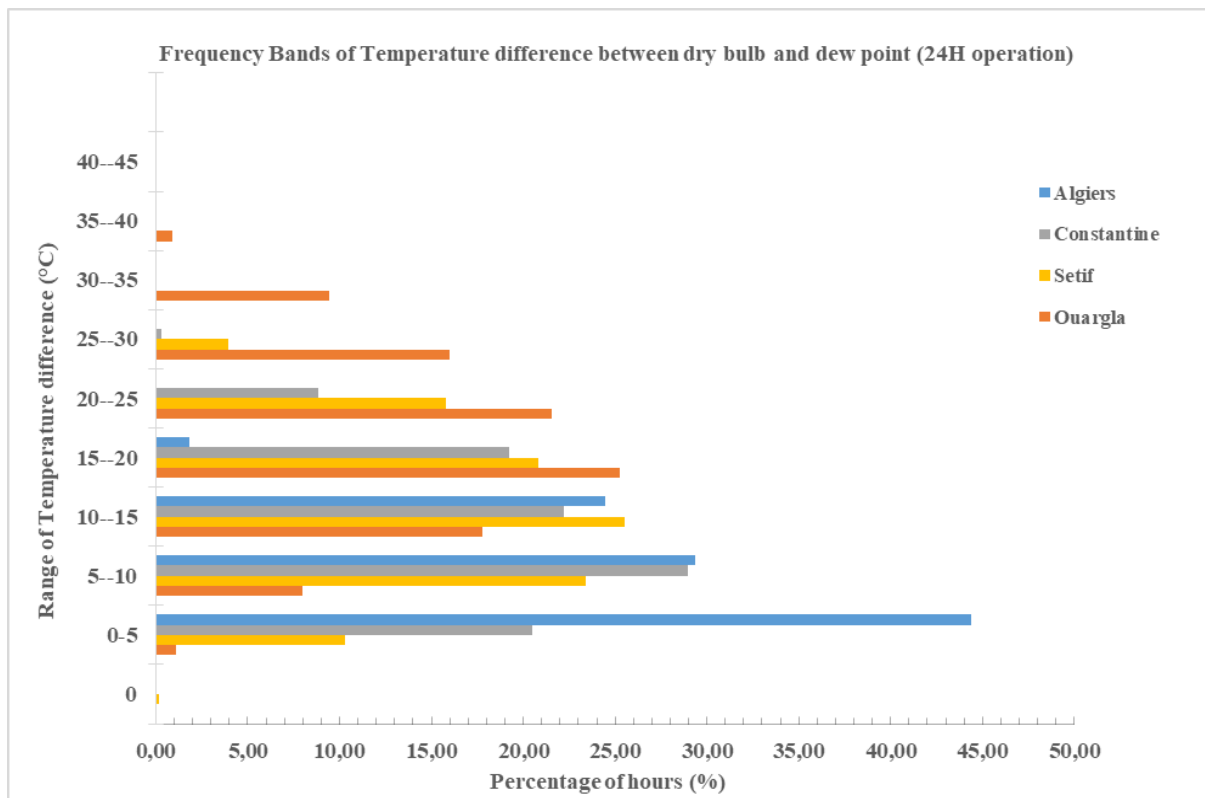
  

$\Delta T = T_{db} - T_{wb} (^{\circ}C)$	Number of Hours	percentage %
<0	0	0.00
0	2	0.14
0-2	184	12.57
2-4	434	29.64
4-6	358	24.45
6-8	228	15.57
8-10	137	9.36
10-12	76	5.19
12-14	38	2.60
14-16	6	0.41
16-18	1	0.07
>18	0	0.00

$\Delta T = T_{db} - T_{wb} (^{\circ}C)$	
<b>Min</b>	0.00
<b>Max</b>	17.00
<b>Average</b>	5.08

The statistical bands/temperature difference frequencies between dry bulb and dew point are shown in figure 7, which indicates that for almost 70-80% of operating hours, the temperature difference falls within the range of 0 - 25°C. These constitute the database used for the design of the dew point system to be used in Algerian climatic conditions. It has been found that a greater value of temperature difference between the dry and the dew point temperature results in greater cooling capacity of the dew point evaporation system.



**Fig.7.** Frequency Bands of Temperature difference between dry bulb and dew point (24 hours operation)

In comparison, Ouargla is drier than Constantine in the hot season. The ambient air temperature is in the range of 13.6 - 48.70°C with an average of 31.43°C. In 62.8% of the time, between May and October, the dry air temperature is in the range of 15 - 30°C. The average temperature difference between the dry bulb and the dew point is 19.90°C. During the day, this average reaches 22.37°C, while in the night it is 16.79°C, which means that a cooling capacity can be reached during the day or during the night. If, for example, the efficiency of the dew point system was 0.7 and the Supply temperature was 22°C, even if the temperature inside was 27°C, the desired set point temperatures would still be obtained.

#### 4. MATHEMATICAL MODEL

To simplify problem analysis, the following assumptions have been made [10,11,14,23]:

- (1) the heat exchanger is adiabatic; there is no heat transfer between system and the surroundings;
- (2) the height of the channels is small compared to their width, thus the flow is

unidirectional; (3) the water film is evenly distributed over the entire surface of the plate; (4) the water and the plate are at the same temperature; (5) the airflow is supposed to be stable and incompressible; (6) the water film is renewed in a constant way ; (7) heat transfer via the channel walls is in the vertical direction.

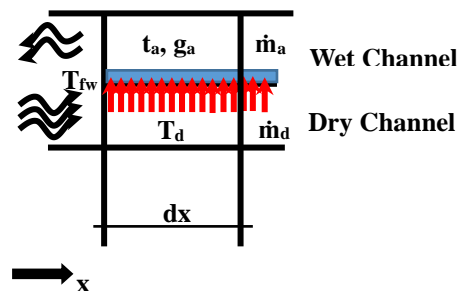


**Fig.8.** Cross Section of calculation element

Taking into account the calculation element shown in Figure 8, the energy conservation balance for the air flow in the dry channel gives:

$$\frac{\dot{m}_d C_{pa}}{D} \frac{dT_d}{dx} = -U_d(T_d - T_{fw}) \quad (1)$$

Where ( $T_d$ ) is air dry bulb temperature in the dry channel, ( $T_{fw}$ ) water film surface temperature, ( $U_d$ ) the overall heat transfer coefficient between the dry channel and water film, ( $D$ ) channel width and ( $\dot{m}_d$ ) airflow rate in the dry channel.

The energy conservation balance for the airflow in the wet channel gives:

$$\frac{\dot{m}_a C_{pa}}{D} \frac{dt_a}{dx} = -h_{aw}(T_{fw} - t_a) - \rho h_m (g_{fw} - g_a) C_{pv} t_a \quad (2)$$

Where ( $t_a$ ) is air-dry bulb temperature in the wet channel, ( $g_a$ ) is the humidity ratio of air (kg/kg<sub>d</sub>) and ( $g_{fw}$ ) is humidity ratio at saturation near water film. The difference between both humidity ratios is the driving force of water evaporation in the wet channel. ( $\dot{m}_a$ ) is airflow rate in the wet channel. ( $\rho$ ) is mass density of humid air, ( $h_{aw}$ ) is the heat transfer coefficient in the wet channel and ( $h_m$ ) is the convective mass transfer coefficient between the wet airflow and the water film surface. They are related by the Lewis relation:

$$\frac{h_{aw}}{h_m} = \rho C_p L e^{2/3} \quad (3)$$

Applying the mass conservation equation to the air in the wet side of the computational channel gives:

$$\frac{\dot{m}_a}{D} \frac{dg_a}{dx} = -\rho h_m (g_{fw} - g_a) \quad (4)$$

Considering the energy balance of a coupled dry and wet element on the media between the channels gives:

$$\frac{\dot{m}_{fw} C_{pfw}}{D} \frac{dT_{fw}}{dx} = -U_d (T_d - T_{fw}) + \rho h_m (g_{fw} - g_a) h_{fg} + h_{aw} (T_{fw} - t_a) \quad (5)$$

To solve this system of equations, the Simulation Problem Analysis and Research Kernel (SPARK) is used, it allows solving efficiently differential equation systems [21]. The equations system was discretized using the finite difference method and the physical system was divided into 20 computational elements.

## 5. RESULTS AND DISCUSSION

### 5.1. Model Validation

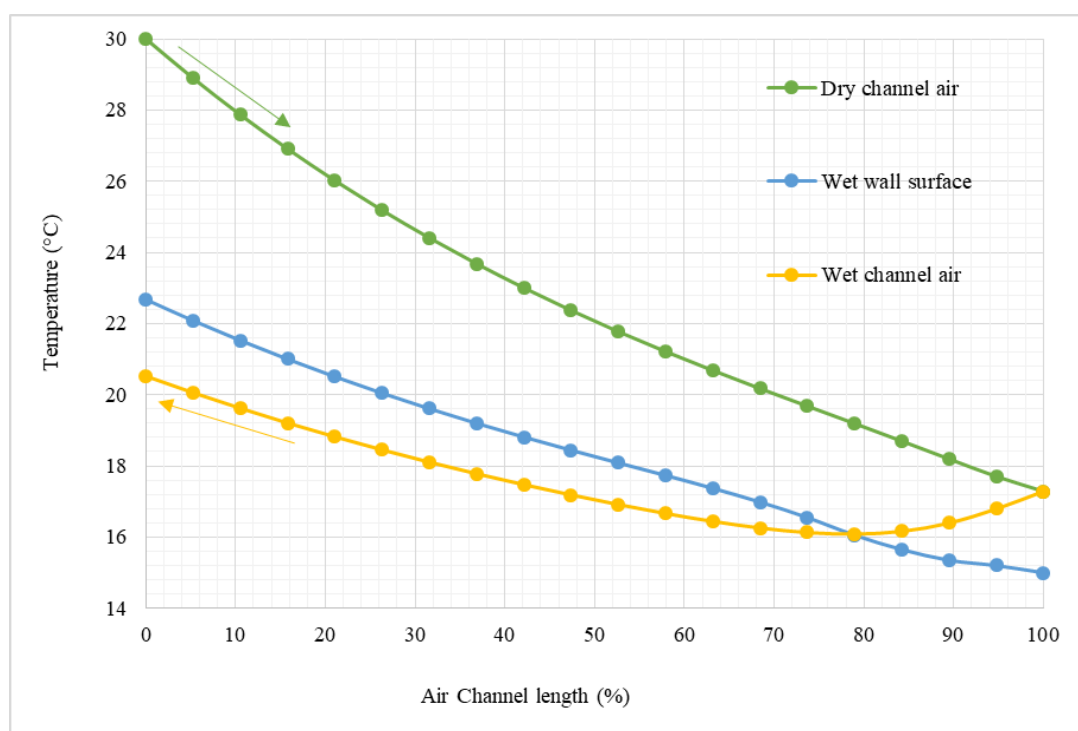
To validate the numerical model, the simulation was carried out on the basis of a similar dew point cooling module, of which the results have been published, either numerically or experimentally [10,11]. Table 5 shows the cooler parameters used in each of these studies as well as the climatic conditions of the intake air.

**Table 5.** Cooler parameters and climatic conditions used in the published data

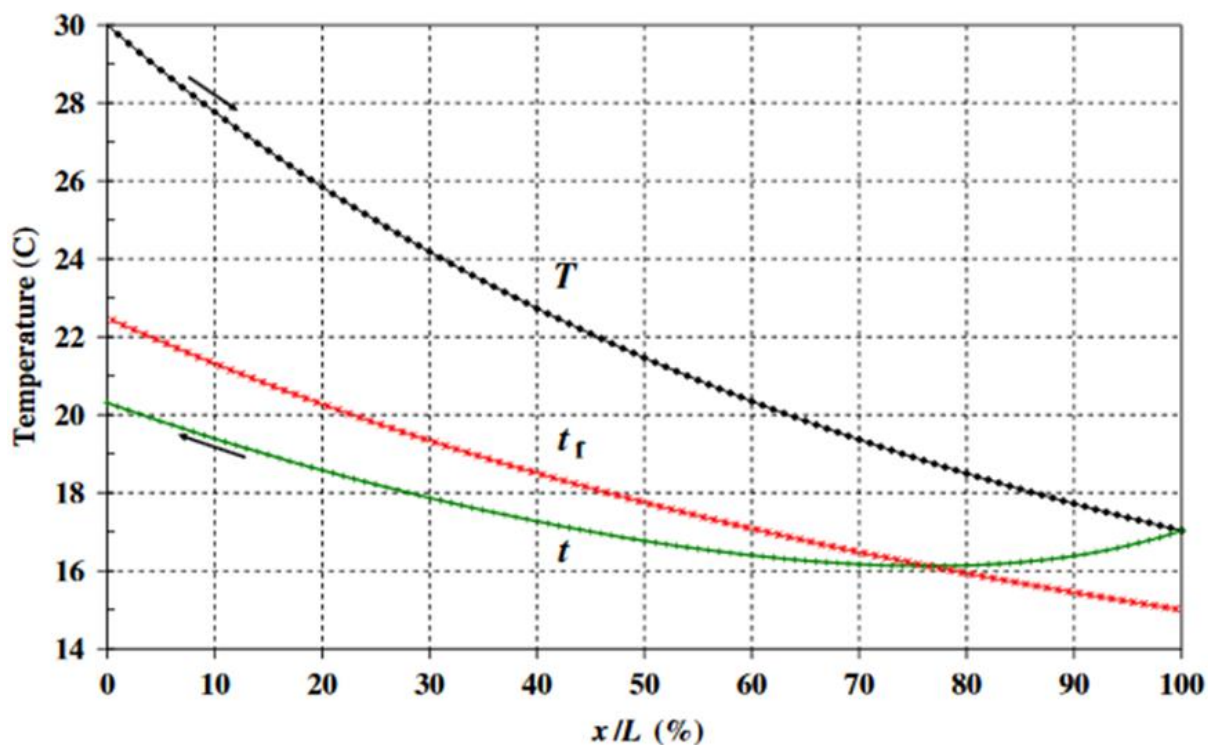
Parameters	Hasan [10]	Riangvilaikul [11]
Channel length (m)	0.5	1.2
Channel width (m)	0.5	0.08
Channel gap (m)	0.0035	0.005
Velocity of inlet ( $\text{m.s}^{-1}$ )	0.676	2.4
Working air ratio	0.7	0.33
Inlet air temperature ( $^{\circ}\text{C}$ )	30	25-30-35-40-45
Inlet air humidity ratio( $\text{g/kgd}$ )	9	6.9-11.2-20-26.4

Figure 9 shows dynamic simulation profiles for the air temperature in the dry and wet channels as well as the surface temperature of the wet wall. These results are obtained from the SPARK model applied to the Hasan case study [10]. The air in the dry channel flows from the opposite side of the air in the wet channel.

It can be noted that the temperature of the intake air falls from  $30^{\circ}\text{C}$  to  $17.3^{\circ}\text{C}$  in the dry channel, which is lower than the temperature of the wet bulb ( $18.8^{\circ}\text{C}$ ).

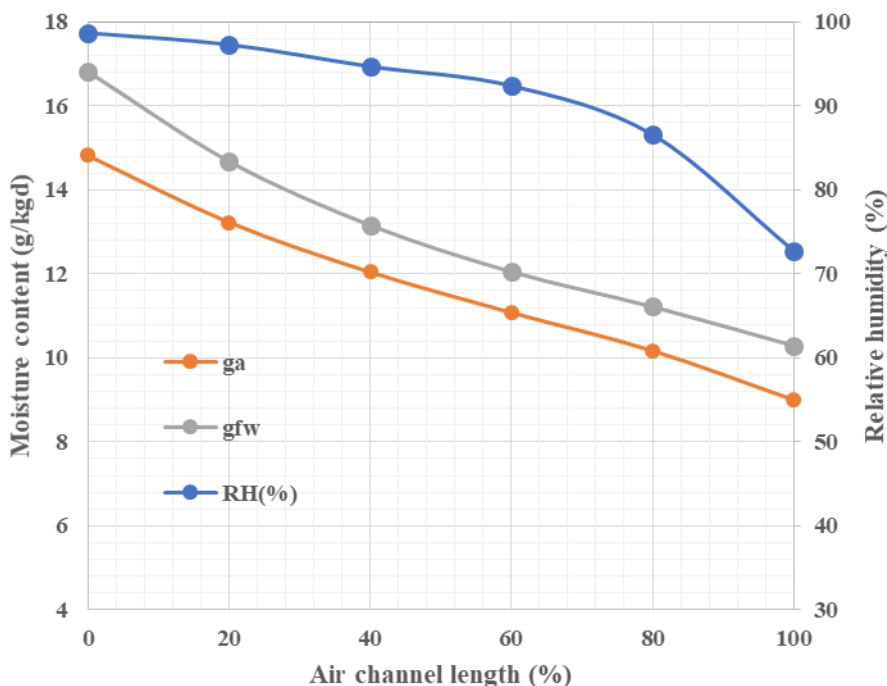
**Fig.9.** Temperature profiles for dry and wet channel given by SPARK

For the wet channel, the working air enters at 17.3°C, its temperature continues to drop for a short initial stage (about 20% of the length of the channel) due to the low temperature of the water on the wet wall surface, then it begins to increase due to heat transfer from the dry channel. Regarding the temperature of the surface of the wet wall, it continues to increase with the air flow in the wet channel because of the heat from the dry channel.



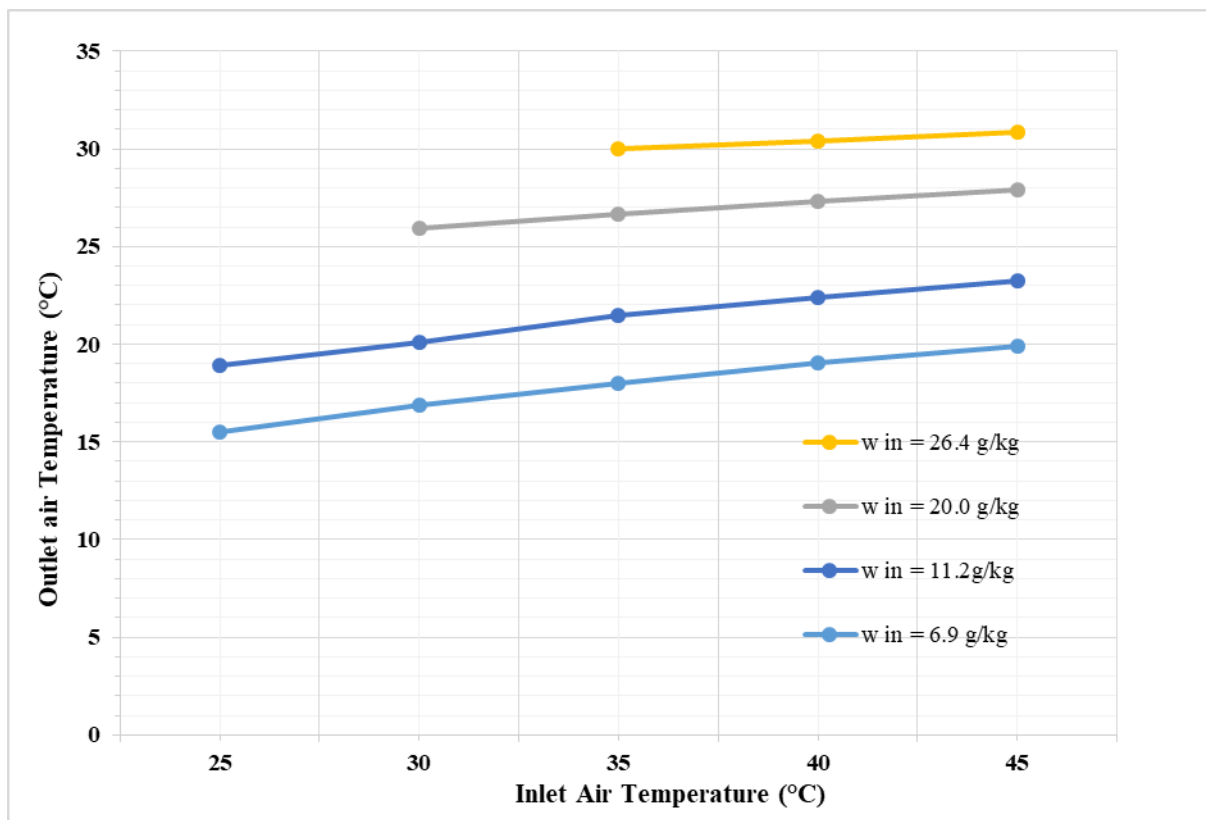
**Fig.10.** Temperature profiles given by Hasan in the Dry Channel, Wet Wall Surface and Wet Channel respectively [10]

Figure 10 represents the data obtained by Hasan [10]. A correspondence is found with those shown in Figure 7 for the results obtained with SPARK. In this case, the air is supplied at 17°C, a difference of 0.3°C with SPARK or a value of 1.76%.



**Fig.11.** Moisture content (g) and Relative Humidity (RH) in the wet channel as computed by SPARK

Figure 11 shows the relative humidity and the moisture content of the air in the wet channel  $g_a$  as well as the saturation moisture content at the wet wall temperature  $g_{fw}$ . The channel length of 100% corresponds to the inlet of the wet channel and the 0% corresponds to the outlet. The moisture content goes from 9 g.kgd<sup>-1</sup> at the entry of the wet channel to 14.82 g.kgd<sup>-1</sup> at its outlet, which indicates that the air leaves the wet channel completely saturated. The difference ( $g_{fw} - g_a$ ) is the driving force behind the evaporation of water in the channel. These results are also validated by the data obtained by Hasan.



**Fig.12.** SPARK numerical results for different inlet air conditions

Figure 12 shows the results obtained by SPARK using the experimental conditions studied by Riangvilaikul and Kumar [11] for different temperatures of intake air and different humidity levels. Increasing the temperature and humidity of the inlet air increases the temperature of the outlet air. On average, a change of 10 g/kg of inlet humidity can cause a change of 6.3°C in the outlet temperature while a change of 10°C in the temperature of the inlet air gives a difference of about 1.59°C. Thus, the main important factor affecting the state of the outlet air is the humidity of the inlet air and the results obtained are in agreement with those reported in scientific literature [11]. Also, for high humidity levels, the error is around 4% due to the lack of information on the conditions of use and the characteristics of the water in this experiment. Our results suggest that the model is in agreement with the published results and that it can therefore be used as a basis for an evaluation and optimization of the system efficiency.

## 5.2. Parametric Analysis

with the intention to develop and design an efficient system, a parametric study is carried out in order to determine the effect of the length of the channel, the temperature of the water at



the inlet of the wet wall and the secondary (working) air ratio (mass report of the airflow in the wet channel to that of the dry channel) on the temperature and humidity of the supply air. For this case, we have taken into account the air inlet conditions of 35°C and a relative humidity of 40% that can be during hot weather in the north of Algeria. The reference case is the same as that studied by Riangvilaikul and Kumar [11] and shown in Table 5. The water inlet temperature at the surface of the wet wall is 21°C. The efficiency of the cooler is evaluated based on its dew point cooling efficiency and its wet bulb cooling efficiency defined as:

$$\epsilon_{dp} = \frac{T_{in} - T_{out}}{T_{in} - T_{dp}} \tag{6}$$

$$\epsilon_{wb} = \frac{T_{in} - T_{out}}{T_{in} - T_{wb}} \tag{7}$$

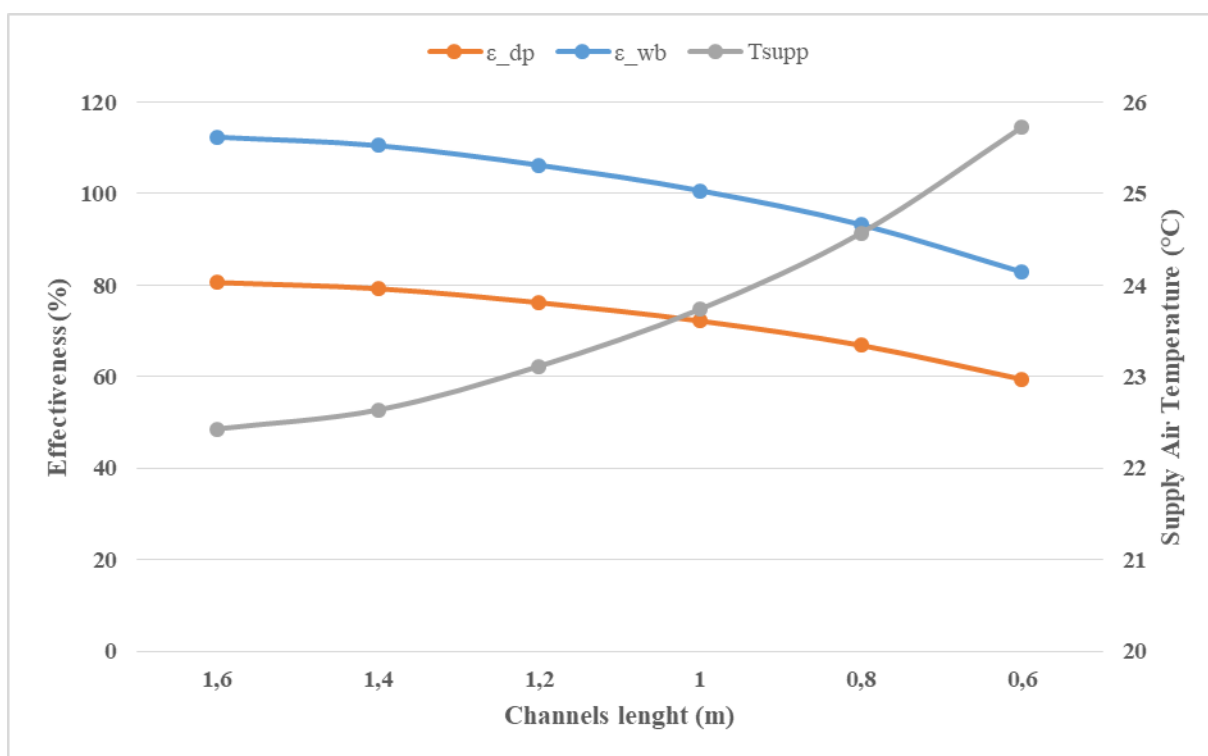


**Fig.13.** Cooling effectiveness and supply air temperature versus channel length

Figure 13 illustrates dew point and wet bulb effectiveness and supply air temperature function

of channel length. In effect, as the shorter this latest, the lesser the wet bulb effectiveness gets and the higher supply air temperature is registered (from 22.43°C to 25.72°C). For instance, when channel length varies from 1.2 to 0.6m dew point effectiveness decreases from 80.6 to 59.45% whereas wet bulb effectiveness decreases from 112.4 to 82.9%. A length greater than 1 m can give a wet bulb efficiency greater than 100%. However, this increase is accompanied by an accentuation in the energy consumption of the fan to overcome the additional resistance due to the channel. As a summary, it could be confirmed that dew point effectiveness decreases slower than wet bulb effectiveness.

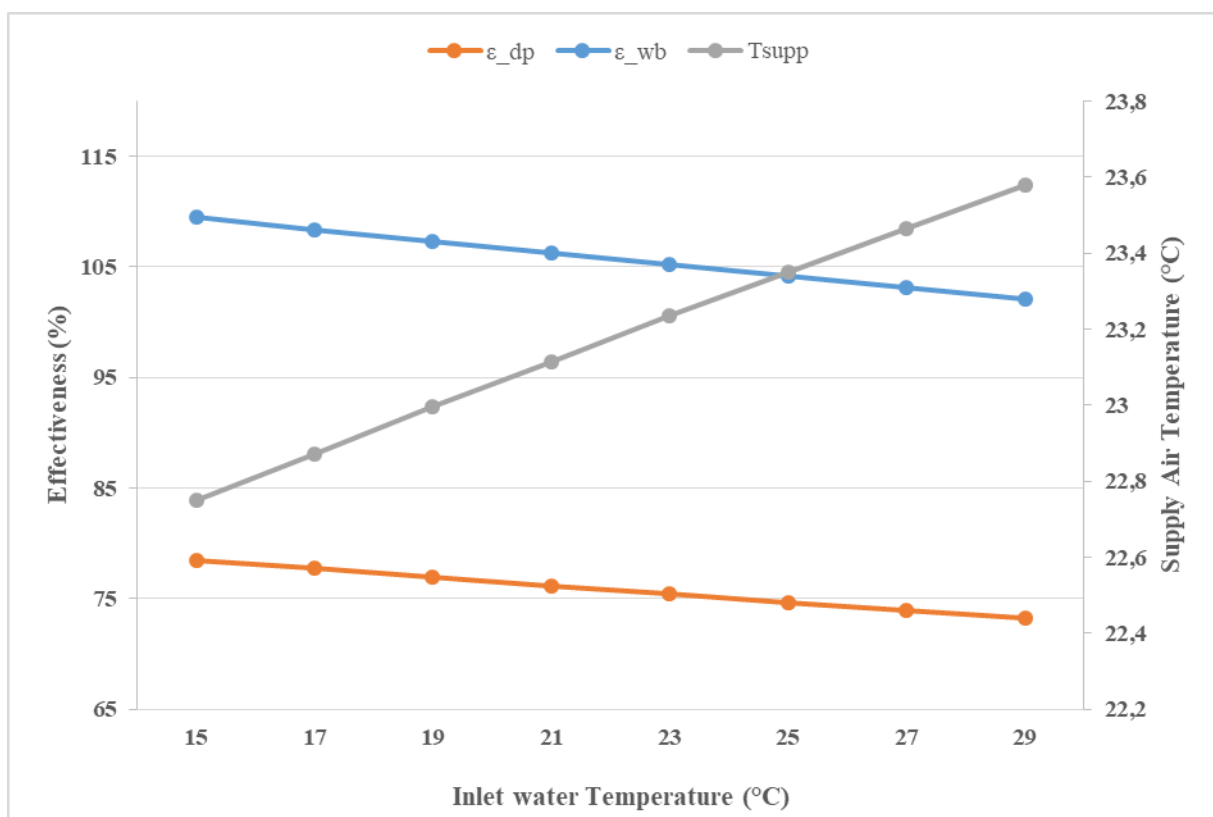


**Fig.14.** Cooling effectiveness and supply air temperature as a function of water temperature

Figure 14 shows the efficiency of the dew point and the wet bulb and the temperature of the supply air based on the temperature of the water at the inlet of the wet wall surface. When the water temperature varies from 15°C to 29°C, the supply air temperature rises from 22.75°C to 23.6°C, which represents an increase of 0.85°C. The efficiency of the dew point  $\epsilon_{dp}$  drops from 78.5 to 73.2% and the efficiency of the wet bulb  $\epsilon_{wb}$  declines from 109.5 to 102% only. These results imply that the effect of water temperature is weak.

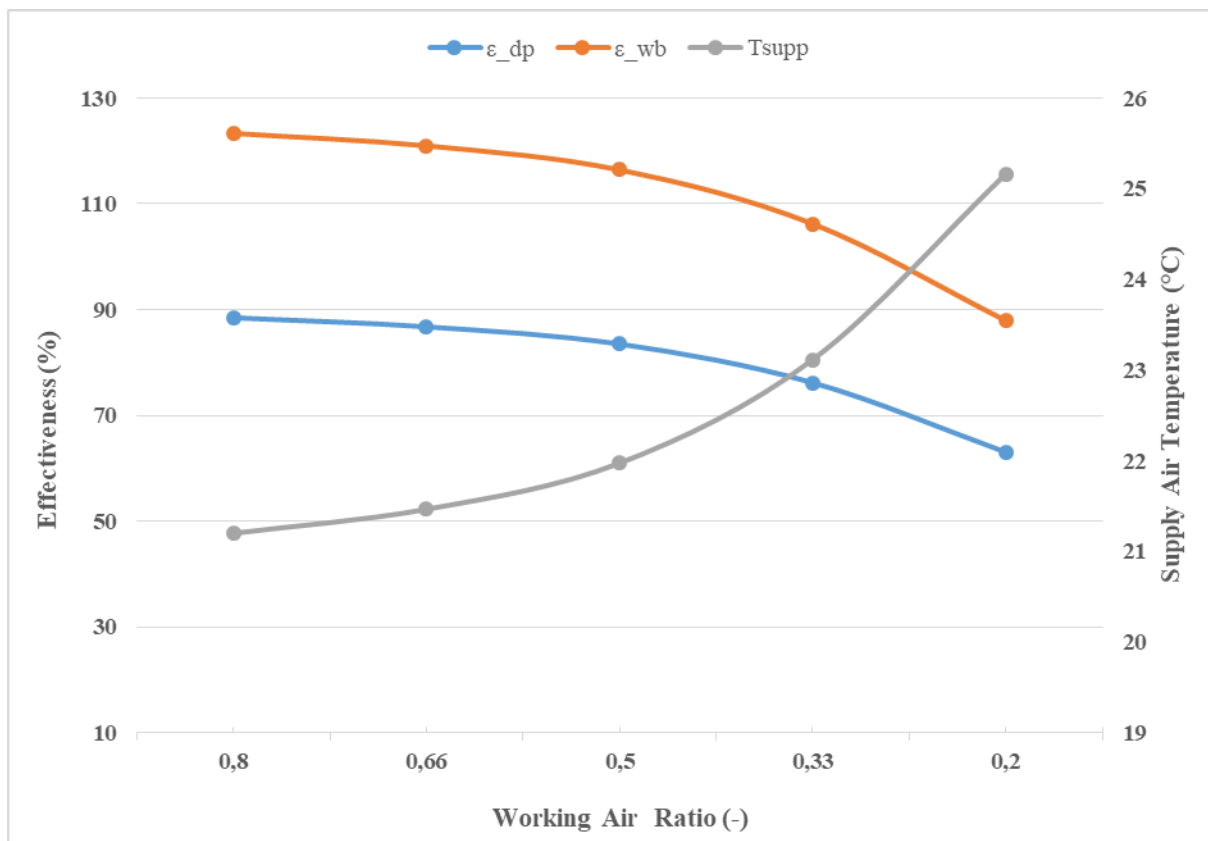


**Fig.15.** Cooling effectiveness and supply air temperature as a function of working air ratio

Figure 15 shows dew point and wet bulb effectiveness and supply air temperature versus working air ratio. Lower working to intake air ratio worsens water evaporation and deteriorates cooler effectiveness however it increases supplied airflow rate and thus can accentuate the system cooling capacity. When working air ratio decreases from 0.8 to 0.2, air supply temperature increases from 21.2°C to 25.16°C. For a ratio lower than 0.3,  $\epsilon_{wb}$  is lower than 100%. For values greater than 0.6, the dew point and wet bulb efficiencies increase slowly, which means that the best suited values to this ratio must be at least 0.3 and not exceed 0.7.

These results show that for the cooler to be effective, its channel length should be higher than 1 m and its working air ratio higher than 0.3.

**5.3. Study of Dew Point Evaporative System Potential under more critical climatic conditions:**

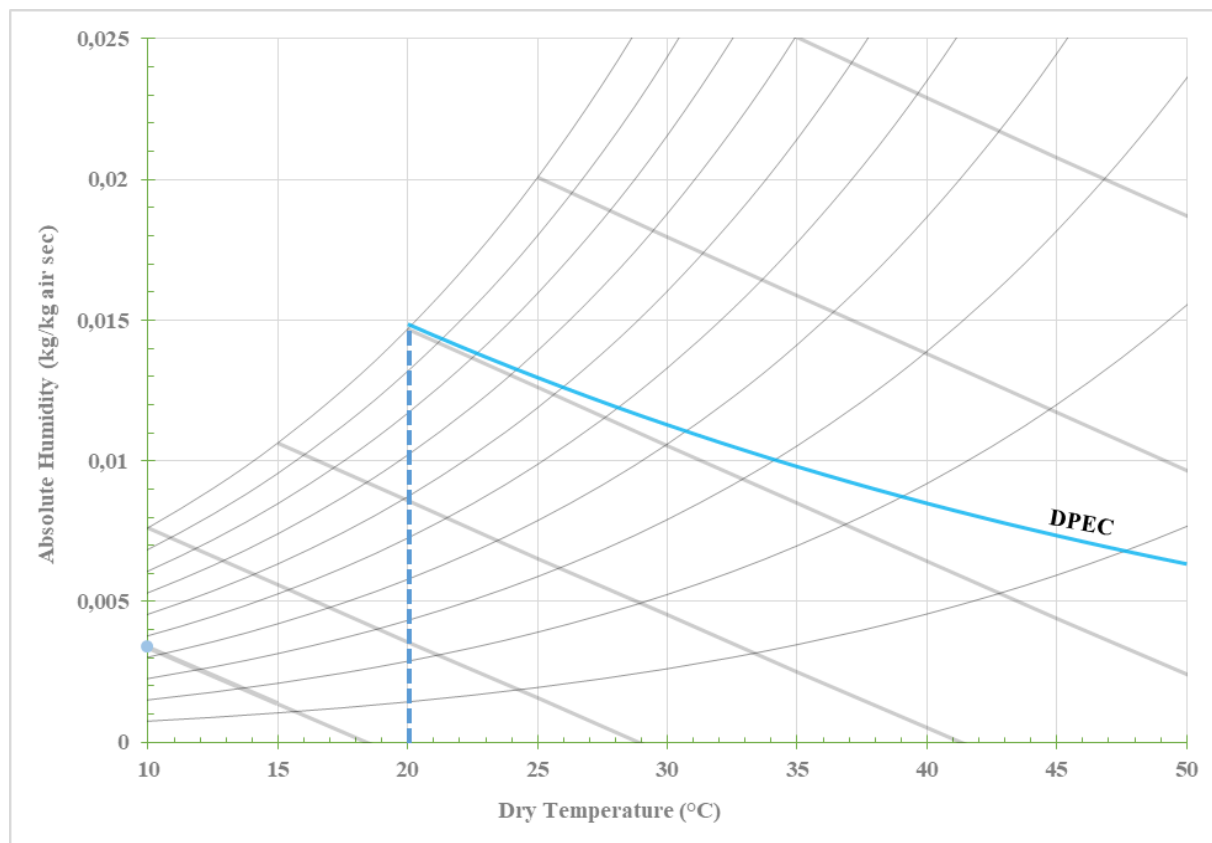
The influence of efficiency on cooling capacity is studied in relation to external air conditions

---

and other parameters specific to the system. The Potential use of the system has been analysed under more severe climate conditions of its performance. In effect, a further investigation in the form of a comparison between Constantine versus Ouargla, a hot and arid location provided further proofs that the choice of the operating mode depends on the external conditions and the required supply air temperature. We will also use the psychrometric chart to show the influence of the various parameters and to delimit the operating conditions of the system. In order to delimit the operation of the device, the boundary line method is used, a line is drawn in the Psychrometric Chart which delimits the external air conditions from which the supply air can be cooled to a minimum given temperature. If the external air condition is above this line, it cannot be cooled to the desired supply temperature. On the other hand, if it is below this line, it can be refreshed at a lower temperature. This is a simple way to describe the potential and limitation of evaporative systems [22].

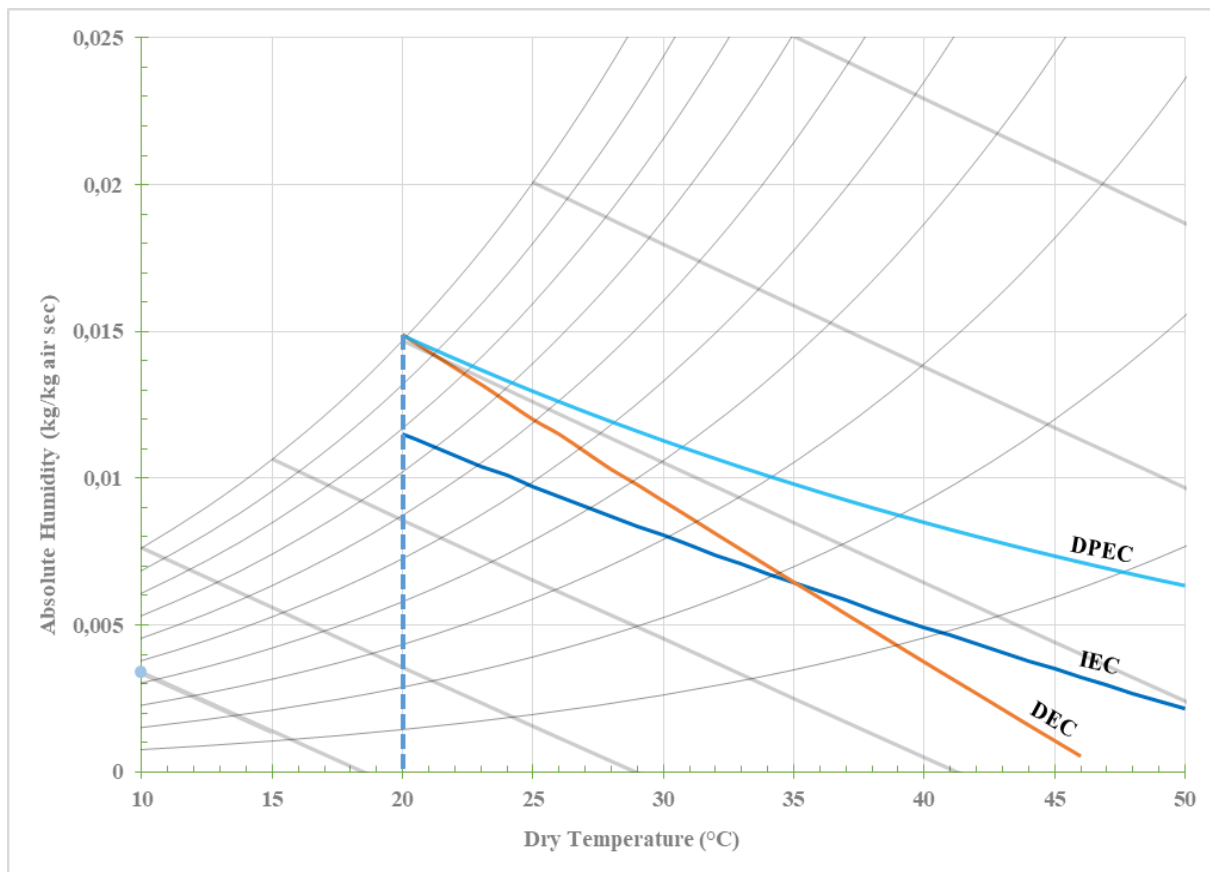
we choose a reference case, we consider a supply air temperature (20 °C), from which we will draw the limit line before changing the parameters in order to study their influences on it.

A room temperature of 25°C was taken as a reference and the rate of the sensible intakes is 0.8 [ $SHR = Q_s / (Q_s + Q_L)$ ]. The efficiency of the exchanger is 0.8. the evaporative coolers have an efficiency of 0.7 for the dew-point mode, and 0.9 for the direct and indirect modes. The supply air temperature is 20°C for direct, indirect and dew-point modes, all at an equal atmospheric pressure of 101325 Pa.



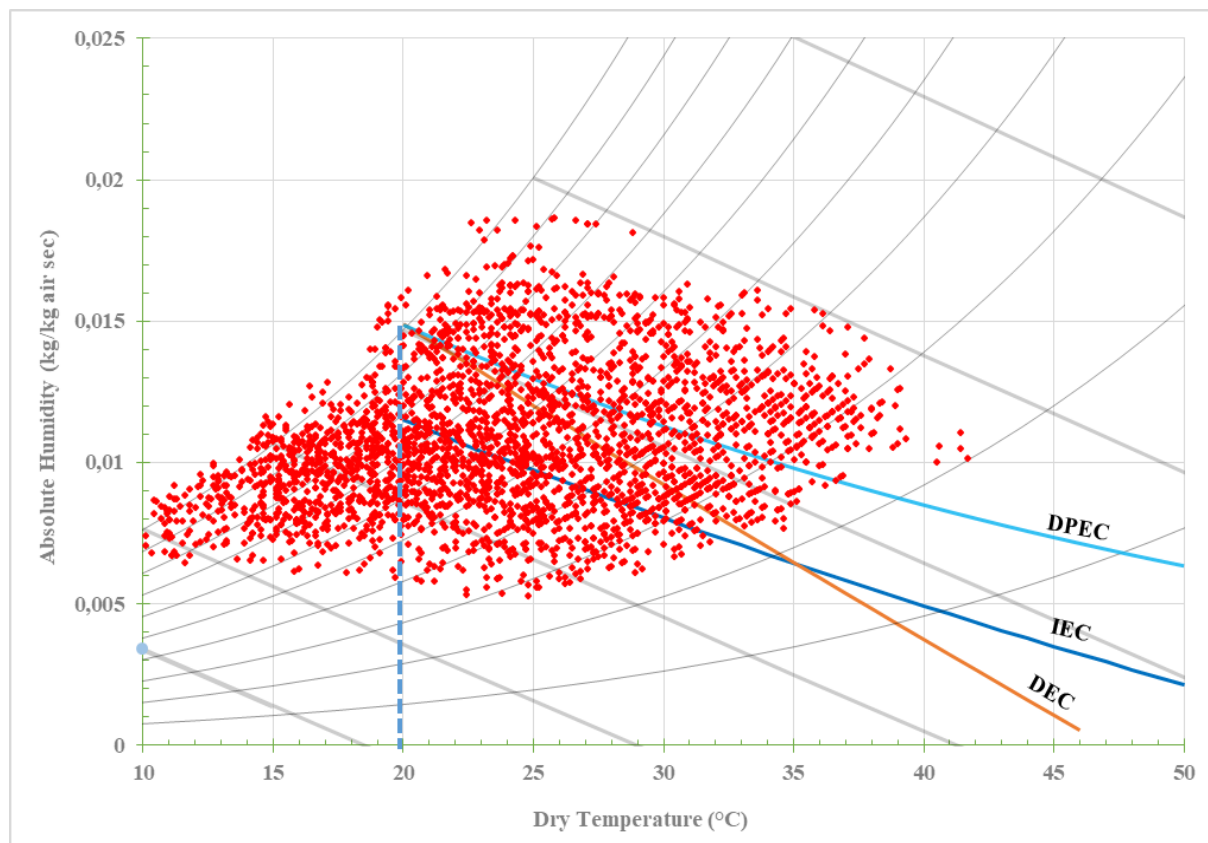
**Fig.16.** The limit line for a DPEC system with efficiency = 0.7 and a supply air temperature of 20 °C

Figure 16 shows the limit line for the reference case for a dew point evaporative cooler system allows to cool the air at lower temperatures than the direct or indirect mode, because if these modes are limited by their humid temperatures, the dew-point mode has freed it and is bounded only by its dew point temperature.



**Fig.17.** Limit lines for 3 evaporative systems: DPEC, IEC and DEC

Figure 17 shows the limit lines for the 3 evaporative systems (DEC, IEC and DPEC) and for a supply air temperature of 20°C, under the reference conditions. It is noted that the limit lines of the Direct and Indirect modes intersect at the temperature of 35°C, the reason being that from this point the humid temperature of the room will be lower than the humid temperature of the outside air (assumed that the temperature of the room is 25°C, which is only realistic for fixed ambient room temperature, therefore air-conditioned). We also note that for low or moderate humidity, the direct and indirect systems are sufficient. On the other hand, the higher the absolute humidity, the more the dew point system will be favoured to obtain the desired supply air temperatures.



**Fig.18.** Representation of boundary lines to evaluate the feasibility of the system (DPEC) for Constantine ( $T_{\text{supp}} = 20^{\circ}\text{C}$ )

Figure 18 shows the climatic conditions for the city of Constantine which is characterized by a less humid continental Mediterranean climate so there is no need for the use of a dehumidification system. We notice that the more we change the operating mode the more the air states are located to the left of the limit line. The indirect mode of operation at Dew Temperature is the one that gives the most satisfaction and makes it possible to obtain the reference conditions and a temperature supply of  $20^{\circ}\text{C}$ . But the outside air is not as dry as it should be for optimal system operation.

The prevailing climate of Ouargla is desert or arid implying a lesser presence of moisture in the air, it is drier than other regions of Algeria. In the figure 19, It can be noted that the Indirect operating mode at dew point temperatures is ideal for this region. For an outdoor temperature of  $40^{\circ}\text{C}$  it is always possible to have ambient temperature setpoints with supply temperatures of  $20^{\circ}\text{C}$ .

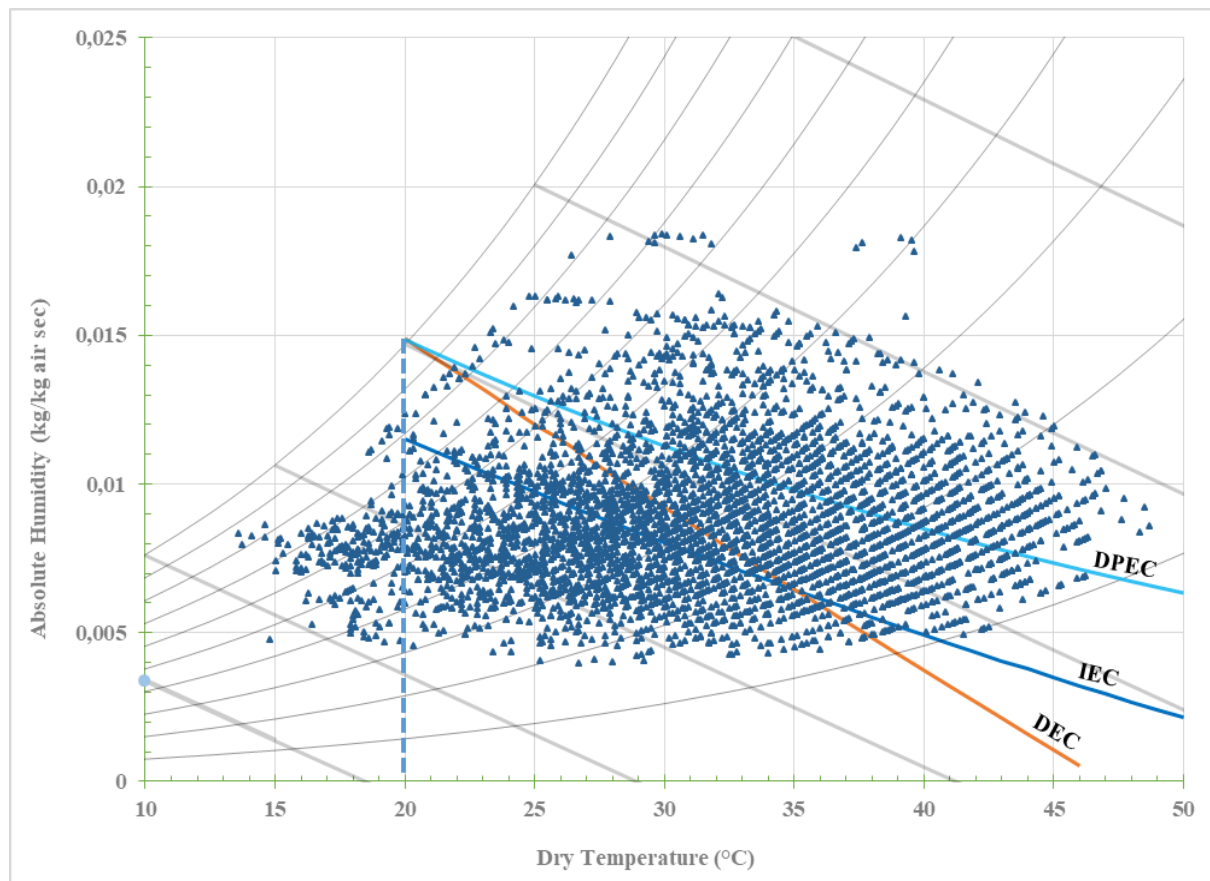


**Fig.19.** Representation of boundary lines to evaluate the feasibility of the system (DPEC) for Ouargla ( $T_{\text{supp}} = 20^{\circ}\text{C}$ )

As in Algeria the supply setpoint temperature is  $25^{\circ}\text{C}$ , with an optimized envelope (which implies reduced external contributions), we can have ambient temperatures of the order of  $27 - 28^{\circ}\text{C}$ , which is reasonable when outside it is  $40 - 45^{\circ}\text{C}$ , even if the air is supplied at  $24 - 25^{\circ}\text{C}$ .

## 6. CONCLUSION

The current investigation indicates that dew point evaporative cooler is able to reduce air temperatures at levels below the wet bulb ambient temperature. A finite difference model of the system was developed based on heat and mass transfer processes. With this model and known input factors, system performance, i.e. supply air quality and cooling efficiency, is predicted. The results obtained during the simulation are promising and in good agreement with the literature outcomes. Simulations are also used to design a cooler system adapted to



Mediterranean climatic conditions. It has been observed that a channel length of at least 1 m and a fresh air intake rate of at least 0.3 would allow a high efficiency of the wet bulb efficiency. Lower humidity results in a greater difference between the dry bulb and the dew point temperatures of the air, which benefits the system by improving its cooling performance. Through the simulation work, the ideal locations for this application were found to be those with a relatively dry and hot climate in summer with relative humidity below 60%. In other areas, north of Algeria, the performance of the dew point system will be reduced due to the relatively lower temperature difference between the dry bulb and the dew point, yet they remain expedient to attain standard indoor thermal comfort. Varying from one location to another, the system cooling capacity is governed by the weather conditions, in particular the dry temperature, humid temperature and the ambient air dew point temperature.

As a subsequent work, these results will be further exploited to validate the outcomes of an experimental prototype assemble to demonstrate the feasibility of the system on site.

One other aim of this research work concerns the reduction of the consumption of electrical energy within the building. The compressor, which is considered the most electricity consumer component in a conventional air conditioning installation, is replaced by a system that revolves around water evaporation to produce fresh air.

Regarding the other devices of the system that consume electricity, such as the pump and the fans, photovoltaic panels could possibly ensure their electricity supply. This will make the installation autonomous and thus allow lesser building energy consumption for air conditioning purposes.

## **7. ACKNOWLEDGEMENTS**

This work is part of the results of a scientific research cooperation between France and Algeria and supported by the Hubert Curien Partnership (PHC TASSILI).

## **8. REFERENCES**

[1] APRUE, 'Consommation énergétique finale : année 2017', Agence Nationale pour la Promotion et la Rationalisation de l'Utilisation de l'Énergie, Alger, Algérie, 2017.

<http://www.aprue.org.dz/documents/Consommation%20énergétique%20finale.pdf>

[2] Enerdata, ‘Tendances de l’efficacité énergétique dans les pays du bassin méditerranéen, Réseau MEDENER, Projet MED-IEE : Indicateurs d’Efficacité Energétique pour la Méditerranée.’, Réseau MEDENER, 2014.

<https://www.medener.org/wp-content/uploads/2017/11/tendances-efficacite-energetique-pays-bassin-mediterraneen-8177.pdf>

[3] R. Belarbi, ‘Développement d’outils méthodologiques d’évaluation et d’intégration des systèmes évaporatifs pour le rafraîchissement passif des bâtiments’, Ph.D. Thesis, University of La Rochelle, France, 1998.

[4] N. Lechner, *Heating, Cooling, Lighting: Sustainable Design Methods for Architects*, 3rd ed. New Jersey, USA: Wiley, 2009.

[5] R. Boukhanouf, H. G. Ibrahim, A. Alharbi, and M. Kanzari, ‘Investigation of an Evaporative Cooler for Buildings in Hot and Dry Climates’, *J. Clean Energy Technol.*, vol. 2, no. 3, pp. 221–225, 2014, doi: 10.7763/JOCET.2014.V2.127.

[6] R. Boukhanouf, A. Alharbi, O. Amer, and H. G. Ibrahim, ‘Experimental and Numerical Study of a Heat Pipe Based Indirect Porous Ceramic Evaporative Cooler’, *Int. J. Environ. Sci. Dev.*, vol. 6, no. 2, pp. 104–110, 2015, doi: 10.7763/IJESD.2015.V6.570.

[7] J. R. Camargo, C. D. Ebinuma, and J. L. Silveira, ‘Thermoeconomic analysis of an evaporative desiccant air conditioning system’, *Appl. Therm. Eng.*, vol. 23, no. 12, pp. 1537–1549, Aug. 2003, doi: 10.1016/S1359-4311(03)00105-4.

[8] C. Maalouf, ‘Etude du potentiel de rafraîchissement d’un système évaporatif à désorption avec régénération solaire’, Ph.D. Thesis, University of La Rochelle, France, 2006.

[9] V. Maisotsenko, L. E. Gillan, T. L. Heaton, and A. D. Gillan, ‘Method and plate apparatus for dew point evaporative cooler’, US6581402B2, 24-Jun-2003.

[10] A. Hasan, ‘Indirect evaporative cooling of air to a sub-wet bulb temperature’, *Appl. Therm. Eng.*, vol. 30, no. 16, pp. 2460–2468, Nov. 2010, doi: 10.1016/j.applthermaleng.2010.06.017.

[11] B. Riangvilaikul and S. Kumar, ‘An experimental study of a novel dew point evaporative cooling system’, *Energy Build.*, vol. 42, no. 5, pp. 637–644, May 2010, doi:

---

10.1016/j.enbuild.2009.10.034.

[12] J. Lee and D.-Y. Lee, 'Experimental study of a counter flow regenerative evaporative cooler with finned channels', *Int. J. Heat Mass Transf.*, vol. 65, pp. 173–179, Oct. 2013, doi: 10.1016/j.ijheatmasstransfer.2013.05.069.

[13] J. Lin, D. T. Bui, R. Wang, and K. J. Chua, 'On the fundamental heat and mass transfer analysis of the counter-flow dew point evaporative cooler', *Appl. Energy*, vol. 217, pp. 126–142, May 2018, doi: 10.1016/j.apenergy.2018.02.120.

[14] R. Boukhanouf, A. Alharbi, H. G. Ibrahim, O. Amer, and M. Worall, 'Computer modelling and experimental investigation of building integrated sub-wet bulb temperature evaporative cooling system', *Appl. Therm. Eng.*, vol. 115, pp. 201–211, Mar. 2017, doi: 10.1016/j.applthermaleng.2016.12.119.

[15] J. Lin, R. Z. Wang, M. Kumja, T. D. Bui, and K. J. Chua, 'Modelling and experimental investigation of the cross-flow dew point evaporative cooler with and without dehumidification', *Appl. Therm. Eng.*, vol. 121, pp. 1–13, Jul. 2017, doi: 10.1016/j.applthermaleng.2017.04.047.

[16] A. Sohani, H. Sayyaadi, and N. Mohammadhosseini, 'Comparative study of the conventional types of heat and mass exchangers to achieve the best design of dew point evaporative coolers at diverse climatic conditions', *Energy Conversion and Management*, vol. 158, pp. 327–345, Feb. 2018, doi: 10.1016/j.enconman.2017.12.042.

[17] J. Lin, D. T. Bui, R. Wang, and K. J. Chua, 'The counter-flow dew point evaporative cooler: Analyzing its transient and steady-state behavior', *Applied Thermal Engineering*, vol. 143, pp. 34–47, Oct. 2018, doi: 10.1016/j.applthermaleng.2018.07.092.

[18] Y. Wan, J. Lin, K. J. Chua, and C. Ren, 'Similarity analysis and comparative study on the performance of counter-flow dew point evaporative coolers with experimental validation', *Energy Convers. Manag.*, vol. 169, pp. 97–110, Aug. 2018, doi: 10.1016/j.enconman.2018.05.043.

[19] Y. Wan, J. Lin, K. J. Chua, and C. Ren, 'A new method for prediction and analysis of heat and mass transfer in the counter-flow dew point evaporative cooler under diverse climatic, operating and geometric conditions', *Int. J. Heat Mass Transf.*, vol. 127, pp. 1147–1160, Dec.

2018, doi: 10.1016/j.ijheatmasstransfer.2018.07.142.

[20] Y. Liu, J. M. Li, X. Yang, and X. Zhao, ‘Two-dimensional numerical study of a heat and mass exchanger for a dew-point evaporative cooler’, *Energy*, vol. 168, pp. 975–988, Feb. 2019, doi: 10.1016/j.energy.2018.11.135.

[21] E. F. Sowell and P. Haves, ‘Efficient solution strategies for building energy system simulation’, *Energy Build.*, vol. 33, no. 4, pp. 309–317, Apr. 2001, doi: 10.1016/S0378-7788(00)00113-4.

[22] C. Maalouf, E. Wurtz, and L. Mora, ‘Effect of Free Cooling on the Operation of a Desiccant Evaporative Cooling System’, *Int. J. Vent.*, vol. 7, no. 2, pp. 125–138, Sep. 2008, doi: 10.1080/14733315.2008.11683805.

[23] P. Xu, X. Ma, and X. Zhao, *A Dew Point Air Cooler toward Super Performance From conception, simulation, fabrication to laboratory testing and applied evaluation*. LAP Lambert Academic Publishing, 2018.

[24] Document Technique Réglementaire DTR C3-2, Réglementation Thermique des Bâtiments d’Habitation, Règles de calcul des déperditions calorifiques, Fascicule 1, Annexe 1, Centre National d’Etude et de Recherches Intégrées du Bâtiment, Ministère de l’Habitat, Algeria.

[25] D. ROUAG. An Investigating of Solar Shading Devices in Algeria. M.Phil. Thesis (Unpublished). School of Architecture and Building Engineering, University of Bath, UK, 1987, P 50-52.

**How to cite this article:**

Abada D, Rouag-Saffidine D, Maalouf C, Polidori G and Sotahi O. Numerical Study and Performance of a Dew Point Evaporative Cooler for Buildings in Constantine, Algeria. *J. Fundam. Appl. Sci.*, 2021, 13(1), 582-617.